Materials Science and Engineering B xxx (2014) xxx–xxx

Contents lists available at ScienceDirect

Materials Science and Engineering B

journal homepage: www.elsevier.com/locate/mseb

Short communication

Influence of metal grid spacing on the conversion efficiency of concentration solar cell at different illumination levels

Q1 Hwen-Fen Hong [a,*], Tsung-Shiew Huang [a], Yen-Yen Chen [b]

[a] Department of Materials Science and Engineering, National Tsing Hua University, 101, Sec. 2, Kuang-Fu Road, Hsinchu 30013, Taiwan
[b] Institute of Nuclear Energy Research, 1000 Wenhua Road, Jiaan Village, Longtan, Taoyuan, Taiwan

ARTICLE INFO

Article history:
Received 25 December 2013
Received in revised form 3 April 2014
Accepted 27 May 2014
Available online xxx

Keywords:
Concentration solar cell
Metal grids
Power loss
Outdoor measurement

ABSTRACT

The design of front metal grid spacing of linear grid pattern for III–V multi-junction concentrated solar cells is a critical issue when high density photocurrent is induced under concentrated sunlight and a poor grid spacing results in resistive losses. In the present work we have performed outdoor experiment and investigated both theoretically and experimentally the effect of ten different metal grid spacing on the electrical performance of high efficiency GaInP/GaInAs/Ge concentrated solar cells under various concentrating level of sunlight. The shadowing ratio of metal grids was adjusted from 3.07% to 6.66%. We have observed that the variation of experimentally obtained variation of power conversion efficiency data with grid spacing is consistent with the variation of theoretical estimation of total power loss with grid spacing. Moreover, the total power loss was dominated by grid shadowing effect at lower concentration levels; while at higher concentration levels the lowest total power loss condition was found when a compromise occurred mainly between grid shadowing effect and resistance of metal lines.

1. Introduction

A concentrating photovoltaic system converts light energy into electrical energy in the same way as conventional photovoltaic technology does. The difference in the technologies is the addition of an optical system that focuses a large area of sunlight onto each concentration solar cell. III–V solar cells under concentrating sunlight are still the state-of-the-art for reaching higher energy conversion efficiencies. In recent years, the efficiency of III–V solar cells has a large progress due to the continuous efforts of some research groups [1–3]. However, the enhancement for energy conversion efficiency for concentrating solar cells is dependent not only on the structure and material of the device but also on the optimization of metal grid pattern and grid spacing [4]. Because the current is so high for concentrator solar cell that appreciable power is lost owing to the various parasitic resistances.

It has been reported that the metal grid pattern has a great impact on the electrical performance of concentrator solar cell. Most researches focused on the theoretical analysis on design optimization of grid of Si solar cells [5–12] and III–V solar cells [13–17], while the experimental demonstrations were rather rare [7]. In the present work, we have designed 10 different metal grid spacing for linear grid pattern to investigate the influence of shadowing effect and series resistance on energy conversion efficiency of multi-junction GaInP/GaInAs/Ge solar cells under different concentration levels. The geometric concentration levels were varied from 200× to 1000×. The effects of four power loss mechanisms of metal grids of solar cells at different illumination intensities were also analyzed. Furthermore, we have performed the outdoor measurement to explore the consistence between theoretically calculated total power loss derived from different power loss mechanisms and experimentally measured energy conversion efficiency data.

2. Basic theories of power losses

When photocurrent generated by junction of solar cell flow to the top emitter, since in the linear grid pattern the grid length is much longer than the grid spacing, it can be assumed that the photocurrent flow laterally in top emitter/window layer and is collected by grid fingers, then flow into busbars [13]. The characteristics of each path can be considered as a resistance and contributes to power loss [14]. There are four power loss mechanisms [6–9] related to metal grid: (1) power loss due to the lateral current flow in the top emitter/window layer ($P_{emitter}$), (2) power loss due to the resistance of contact metal finger (P_{metal}), (3) power loss due to the contact resistance between metal and semiconductor ($P_{contact}$),

Q2 * Corresponding author. Tel.: +886 930 886068.
E-mail address: hfhong@iner.gov.tw (H.-F. Hong).

http://dx.doi.org/10.1016/j.mseb.2014.05.011
0921-5107/© 2014 Published by Elsevier B.V.

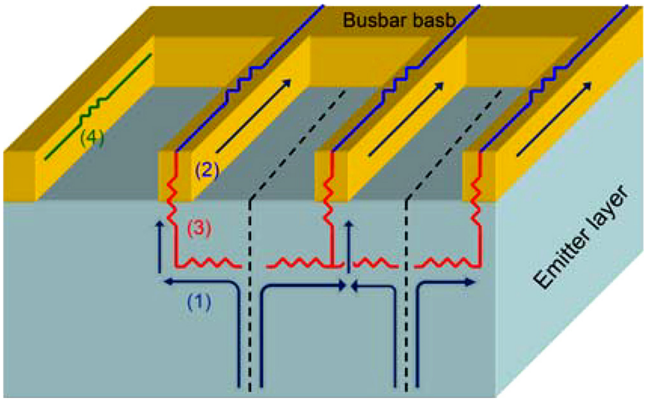

Fig. 1. Schematic illustration of four power loss mechanisms and current flow direction of concentrator solar cell.

and (4) power loss due to the metal grid shadowing (P_{shadow}). Fig. 1 shows the schematic illustration of four power loss mechanisms and the direction of photocurrent of concentration solar cells. To analyze power losses of concentrator solar cells, we used analytical expressions reported in the literature [6–9], and those power losses were calculated according to Eqs. (1)–(4). The meaning of each parameter is listed in Table 1.

$$P_{emitter} = R_{emitter}\frac{J_{mp}S^2}{12V_{mp}} \quad (1)$$

$$P_{metal} = \frac{1}{12}L^2R_{metal}\frac{J_{mp}S}{V_{mp}W_f} \quad (2)$$

$$P_{contact} = \rho_{contact}\frac{J_{mp}S}{V_{mp}W_f} \quad (3)$$

$$P_{shadow} = \frac{A_{metal}}{A_{cell}} \quad (4)$$

3. Experiment

GaInP/GaInAs/Ge triple-junction solar cells were applied in this study. The schematic structure of solar cell is shown in Fig. 2. The active area of the cell is 0.1406 cm^2 (3.75 × 3.75 mm^2), and the materials of metal grid is sequentially deposited 0.8 μm Ni/Ge/Ag alloy and 5 μm Au. To facilitate this investigation, we have designed 10 metal grid spacing of linear grid pattern. The spacing between two adjacent grids is adjusted ranging from 75 μm to 165 μm in an increment of 10 μm. The square solar cell has two busbars at edges and the fingers are perpendicular to busbars as shown in Fig. 3. In this investigation, the solar cell chip was bonded on the printed ceramic substrate with solder, then the printed ceramic substrate was mounted on Al-plate which serves as a heat sink [18,19]. Typically, the solar cell was encapsulated with transparent silicone to prevent from the penetration of moisture into solar cell and suffering contamination. The schematic cross-sectional graph of the sample is shown in Fig. 4. The designed parameters of solar

Table 1
Meaning of each parameter in Eqs. (1)–(4).

R_{metal}	The sheet resistance of the front metal grid finger
$R_{emitter}$	The sheet resistance of the emitter/window layer
$\rho_{contact}$	Specific contact resistance
S	Front grid finger spacing
L	The length of the front grid finger
W_f	The width of the front grid finger
J_{mp}	Current density of maximum power point
V_{mp}	Voltage of maximum power point
A_{metal}	Total area of metal grids
A_{cell}	Total area of cell

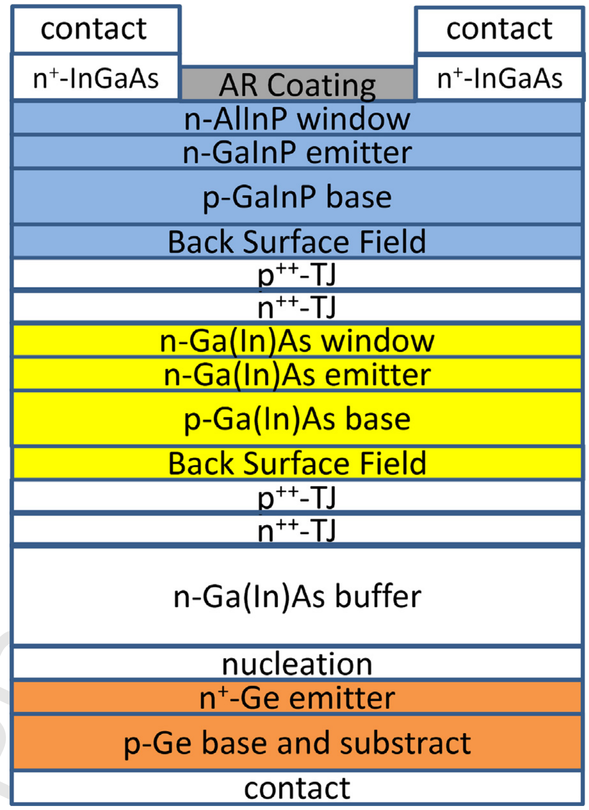

Fig. 2. Schematic structure of GaInP/GaInAs/Ge triple-junction solar cell.

cells are listed in Table 2, the data shown in the rightmost column of table is shadowing ratio for different cells. The active area and the grid width of solar cells is always fixed in 3.75 × 3.75 mm^2 and 5 μm respectively, however the area of Fresnel lens is dependent on the geometric concentration levels. The areas of Fresnel lenses at various concentration levels are listed in Table 3.

Fig. 5 shows a picture of our outdoor measurement system for concentration solar cell, which includes a sun tracker (EKO, Model: STR22), a normal incidence pyrheliometer (Eppley, Model: NIP), and a source meter (Keithley, Model: 2420). The inset photograph shows the packaged solar cell. A sun tracker is used to follow up the sun such that sunlight will incident perpendicularly to Fresnel lens and will be well focused on solar cell. A source meter is employed to measure the characteristic I–V curves, and then to obtain I_{SC}, V_{OC}, I_{mp}, V_{mp} of the solar cell. From the NIP, the in-time direct normal irradiance (DNI) can be recorded and the incident power of sunlight can be obtained. Finally, the energy conversion efficiency, η, can be calculated by the following equation:

$$\eta = \frac{P_m}{P_{in}} = \frac{I_{mp}V_{mp}}{\mathrm{DNI} \times A_{lens}} \times 100\%, \quad (5)$$

here P_m is the measured power, P_{in} is the incident power of sunlight, I_{mp} is current of the maximum power point, V_{mp} is voltage of the maximum power point, and A_{lens} is the area of Fresnel lens.

All the measurements for those 10 samples were performed one-sun as outdoor environment under 200×, 400×, 600×, 800×, and 1000× sunlight illumination. The geometrical concentration ratio (X) is defined as the lens area divided by cell area. It is well known that multi-junction solar cells are quite sensitive to spectrum change [18,19]. Therefore, we carried out the experiments at noon time on a clear-sky day, DNI (direct normal irradiance) 840 ± 20 kW/m^2.

Sheet resistances of NiGeAg/Au metal, R_{metal}, and emitter/window layer, $R_{emitter}$, were measured by a co-linear four point